E-proceedings of the 38th IAHR World Congress
September 1-6, 2019, Panama City, Panama
doi:10.3850/38WC092019-0208

ANALYSIS OF FUTURE PRECIPITATION AND RUNOFF CHANGES IN YA-LUNG RIVER BASIN, CHINA

SIYU CAI(1), WEIHONG LIAO(1), YINMAO ZHAO(2) & JING WU(3)

(1) State Key Laboratory of Simulation and Regulation of Water Cycle in River Basin, China Institute of Water Resources and Hydropower Research (IWHR), Beijing, China
caisiyuchina@163.com; behellen@qq.com
(2) State Key Laboratory of Hydraulic Engineering Simulation and Safety, Tianjin University, Tianjin, China
scirencc@tju.com
(3) Geological Environmental Monitoring Station of QingHai Province, Qinghai, China
783897279@qq.com

ABSTRACT

Using the 10 models of NEX-GDDP CMIP5 to perform equal weighted averaging in the RCP4.5 and RCP8.5 scenarios to obtain daily precipitation data under the multi-model set, and based on this, the spatial characteristics of extreme precipitation events in the Ya-lung River Basin from 2020 to 2099 were carried out. After using the Hargreaves-Samani (HS) method to obtain future evaporation data in the future, the CREST model is driven to simulate the future daily runoff of the Ya-lung River Basin, and the precipitation and runoff changes are analyzed from the interdecadal and seasonal. Finally, the multivariate trend analysis of precipitation and runoff is carried out to provide favorable help for the planning, development and utilization of water resources in the Ya-lung River Basin. The results show that: 1. The annual total wet-day precipitation, the number of heavy precipitation days, the simple daily intensity index and the max 5-day precipitation amount in the two scenarios show a significant increase trend, while the consecutive dry days show opposite changes in the two scenarios. Spatially, the indicators vary. 2. CREST model has good applicability in Ya-lung River Basin. The Nash efficiency coefficient (0.83,0.84), deterministic coefficient (0.84,0.85) and relative error (-2.05% and 3.01%) in the calibration and verification period all meet the accuracy requirements. 3. In both scenarios, the increase in precipitation is mainly concentrated in winter, while the increase in runoff is mainly concentrated in summer and autumn. 4. Under the multivariate trend analysis, the future precipitation and runoff in the Ya-lung River Basin show an decreasing trend under both scenarios.

Keywords: Climate change, Extreme precipitation, Ya-lung River Basin, Trend analysis, CREST model.

1 INTRODUCTION

Climate change has become a pressing issue in the world today and the impact of human activities on the Earth's ecosystem has gained pre-eminence (IPCC, 2007; IPCC, 2013). Climate change and global warming will cause significant changes in the hydrological cycle, resulting in redistribution of water resources in spatiotemporal pattern, and directly affect precipitation and surface runoff, thus, aggravating water resources problems (Chen et al., 2017). The increase in precipitation intensity and variability and seasonal variation in runoff, especially, would increase the risk of floods and droughts, while bringing new challenges into watershed management, flood control, and drought relief. It is crucial to strengthen the study of temporal and spatial patterns of water resources under future climate scenarios to formulate adaptive policies to cope with the impact of future climate change on water resources (Jiang et al.,2007; Xu et al., 2009).

The main way to study the impact of climate change on runoff is to combine climate projections with hydrological models to predict future runoff changes (Yu et al., 2002; Xu et al., 2007; Vaze and Teng, 2011). Yu et al. (2002) used the Semi-distributed Hydrologiska Byrans Vattenbalansavdelning (HBV) model and non-parametric statistical test to simulate future runoff changes in southern Taiwan based on trend analysis of meteorological variables. Their results indicate that the transition probabilities of daily precipitation occurrence significantly influence precipitation generation, and generated runoff for future climatic conditions in southern Taiwan was found to rise during the wet season and decline during the dry season (Yu et al., 2002). Franczyk used the semi-distributed ArcView Soil and Water Assessment Tool hydrological model to simulate future precipitation and runoff in the Portland metropolitan area, Oregon, USA. Their results show that the average annual temperature of the study area will increase by 1.2℃ in future. Compared to the baseline period, the

average annual precipitation will increase by 2%, the average annual runoff will increase by 2.7%, and the summer runoff will decrease by 1.6% (Franczyk and Chang, 2009).

Silberstein et al. (2012) used five simple conceptual rainfall-runoff models to analyze the runoff changes in southwestern Australia under the scenarios of global temperature rise of 0.7, 1.0, and 1.3℃. Their results show that with global warming, the median of rainfall will be 8% lower than the baseline period, resulting in a 25% reduction in the median runoff compared to the baseline period (Silberstein et al., 2012). Because most areas in China are monsoon climates, runoff and precipitation in China are more sensitive to climate change (Wang et al, 2011). The study by Chen et al (2014) shows that different watersheds in China have different responses to the same climate change scenario—the Haihe River Basin has the highest sensitivity. The Yellow River, Huaihe River, Liaohe River, Songhua River, Pearl River, Yangtze River, and Southeast River have lower volume, and their sensitivity to climate shows a decreasing trend (Chen et al., 2014). Meanwhile, the runoff variation characteristics in different watersheds are also different. Based on the projection results of the ECHAM5/MPI-OM model in the two climate change scenarios of A2 and B1, Liu et al. (2009) pointed out that during 2001–2050, glacial runoff will increase in spring and early summer in the source region of Yangtze River, but decreases significantly in late summer (Liu et al., 2009). Moreover, the weakened South China Sea summer monsoon will induce precipitation decrease in the Yellow River in a scenario of global warming and the flows in the source region of Yellow River are likely to decrease in the next 20 years (Li et al., 2012). Similarly, future runoff and precipitation in the Yellow River Basin under IPCC's RCP4.5 scenario also indicates that the trend will decrease compared to the baseline period (Yuan et al., 2018). Yuan et al. conducted a precipitation and flood analysis of the Jinsha River in the southwest China for the next 2020-2050 compared with the basline period from 1960 to 1990. The results show that the water in the RCP4.5 and RCP8.5 scenarios will increase by 1.0%-33.7% compared to the baseline period, the change of extreme floods relative to the base period is 0.8% - 23.8% and - 6.2 - 28.2% (Yuan et al., 2018).

The above research is mainly concentrated in the Yellow River and the Yangtze River basin. There are few concerns and researches on the Ya-lung River basin with many hydropower stations and abundant water resources. Many reservoirs and power stations in the Ya-lung River Basin constitute a complex engineering system that affects the safety of the power system in the southwest China. Future precipitation and changes in runoff play a decisive role in the hydroelectric energy of the Ya-lung River and affect the spatial and temporal distribution of water resources. Detailed, systematic and complete prediction of precipitation characteristics, extreme precipitation events and runoff are not only important for engineering design and making adaptation policies for hydrology and water resources, but also for the planning, development and utilization of water resources in the Ya-lung River Basin (Supari et al., 2017).

Based on 10 CMIP 5 high-resolution model prediction from NASA Earth Exchange/Global Daily Downscaled Projections (NEX-GDDP) under two scenarios (RCP4.5 and RCP8.5), the extreme precipitation events and the variation characteristics of precipitation and runoff in the Ya-lung River Basin are analyzed using multi-model ensemble prediction. The main contents of the study are as follows. a) The temporal and spatial distribution and variation trend of extreme climate indices for precipitation in future climate scenarios are analyzed using a set of extreme climate indices recommended by the Expert Team on Climate Change Detection and Indices (ETCCDI). b) After verifying the applicability of the Coupled Routing and Excess Storage (CREST) model in Ya-lung River Basin, using the results of the multi-model set, CREST is employed to simulate the runoff from 2020 to 2099 and the precipitation and runoff in Ya-lung River Basin are analyzed on interdecadal scale with the baseline period 2005–2014. c) A comprehensive analysis of the multivariate indicators of runoff provides a basis for future flood disaster analysis in the Ya-lung River Basin.

2 RESEARCH AREA AND METHOD

2.1 Study area

The Ya-lung River originates from the southern foothills of Bayan Kala Mountain in Qinghai Province and flows through Qinghai, Sichuan and other provinces. It is a tributary of the Jinsha River in the upper reaches of the Yangtze River. The main stream of the Ya-lung River is 1571km long and the drainage area is 144,000 square kilometers (Figure 1). The Ya-lung River basin belongs to the western Sichuan plateau climate zone. The rainfall is 600-800 mm in the upstream zone, 1000-1400 mm in the middle zone and 900-1300 mm in the downstream zone. The runoff of the Ya-lung River is mainly formed by precipitation, and the rest is replenished by groundwater and snowmelt and icemelt. The runoff has little change in the interdecadal period. The average annual flow of the watershed outlet is 1890 m^3/s, the annual runoff is 596×10^8 m^3, and the runoff in the wet season (June to October) accounts for 77% of the whole year (Yang et al., 2018).

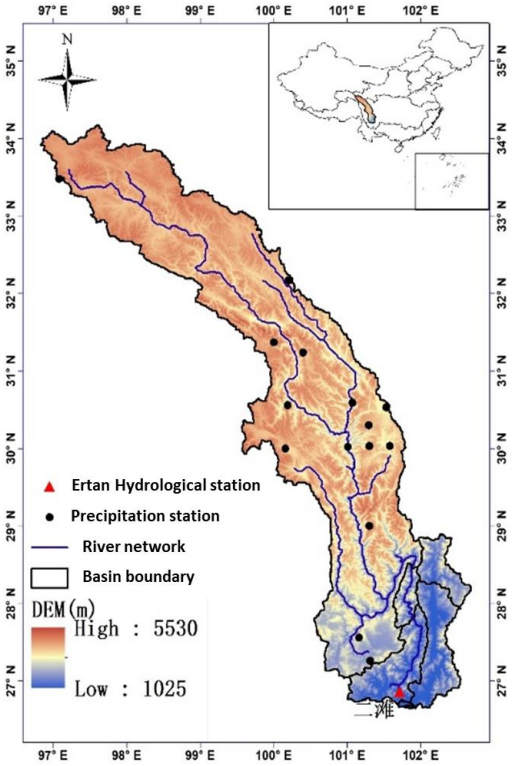

Figure 1. Geographical location of the study area.

2.2 Research method

2.2.1 CREST hydrological model

CREST is a grid-based distributed hydrological model jointly developed by the University of Oklahoma and NASA. It can combine satellite remote sensing data and observational data for local, regional, and global hydrological analysis (Tang et al., 2016).

The overall framework of CREST V2.1 is shown in Figure 2. The data needed for the operation of the model are digital elevation model (DEM), flow accumulation map (FAC), flow direction map (FDR), digital river network, and slope. DEM, FAC, and FDR are all raster format. The output data of the model mainly include daily runoff of hydrological stations at the basin outlet, and evapotranspiration, free water storage capacity, precipitation, and surface runoff in the basin.

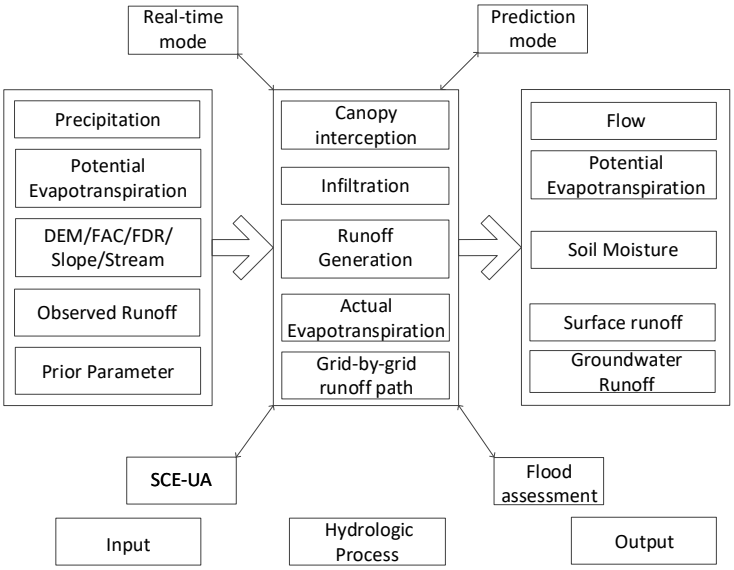

Figure 2. CREST model structure.

Currently, CREST is used for global scale research (KHAN et al., 2011; KHAN et al.,2011 ; Huan et al., 2012). In this study, Nash efficiency coefficient (Nash), certainty coefficient (R2), and bias (Bias) were chosen to evaluate the simulation effect of the model in the calibration and validation periods. The consistency between the observed value and simulated value is determined by R^2. The values generally range from 0 to 1.0, where

the higher values indicate less error variance and the values greater than 0.50 are generally recognized as acceptable. Furthermore, Nash is employed to predict the relative values. These range between -∞ and 1.0 with Nash, which is an optimal value when it is equal to unity. The simulation model is considered satisfactory if the value of Nash>0.5 and Nash greater than 0.8 denotes better simulation results (Nilawar and Waikar, 2018).

$$\text{Nash} = 1 - \frac{\sum_{i=1}^{n}(QS_i - QO_i)^2}{\sum_{i=1}^{n}(QO_i - \overline{QO})^2} \quad [1]$$

$$R^2 = \left(\frac{\sum_{i=1}^{n}(QS_i - \overline{QS_i})(QO_i - \overline{QO_i})}{\sqrt{\sum_{i=1}^{n}(QS_i - \overline{QS_i})^2 \sum_{i=1}^{n}(QO_i - \overline{QO_i})^2}}\right)^2 \quad [2]$$

$$\text{Bias} = \frac{(QS_i - QO_i)}{QS_i} \times 100\% \quad [3]$$

where: QS_i is the simulated runoff value for period i, QO_i is the measured runoff value for i period, $\overline{QO}$ is the average value of measured runoff, and i=1, 2, 3, ..., n.

2.2.2 Extreme climate indices for precipitation

The extreme precipitation index recommended by ETCCDI (Expert Team on Climate Change Detection and Indices) has high stability and intuitive calculation and interpretation ability, so it is widely used in climate research and related fields (Wang et al., 2017). In this study, we selected seven representative precipitation extreme climate indices recommended by ETCCDI to analyze the characteristics of precipitation in the Ya-lung River basin and the temporal and spatial distribution and variation trend of extreme climate indices for precipitation in future climate scenarios. Table 2 lists the names and definitions of the indices computed in this study (Cheng et al., 2013; Filahi et al., 2016).

Table 1. Information on the 7 indices used in this study.

Label	Index name	Index definition	Units
PRCPTOT	Annual total wet-day precipitation	Annual total precipitation in days ≥ 1 mm	mm
SDII	Simple daily intensity index	The ratio of annual total precipitation to the number of wet days (≥ 1 mm)	mm/day
R1mm.	Number of precipitation days	Annual count of daily precipitation ≥1 mm	days
RX5day	Maximum 5-day precipitation volume	Annual maximum consecutive 5-day precipitation	mm
R10mm	Number of heavy precipitation days	Annual count of precipitation ≥10 mm	days
CDD	Consecutive dry days	Maximum number of consecutive days of precipitation < 1 mm	days
R95p	Strong precipitation events	Fraction of annual total precipitation due to events exceeding the 1961–1990 95th percentile	

3 DATA COLLECTION PROGRAM

3.1 Precipitation data

China gauge-based daily precipitation analysis product (CGDPA) was used as the precipitation reference data in this study. CGDPA is developed by the National Meteorological Information Center of China Meteorological Administration using the “climate background field” optimal interpolation method to grid the daily precipitation data of more than 2,400 stations nationwide. The spatial resolution of CGDPA’s is 0.25° × 0.25°, and the precision and reliability has been proved (Shen et al.,2014). Shen et al. (2016) have validated the accuracy of Climate Prediction Center Unified Gauge (CPC_UNI) data and CGDPA data based on independent precipitation observations. Their results show that CGDPA has lower deviation and root mean square error and higher spatial correlation coefficient compared with CPC_UNI data, which can be used as the input data for hydrological applications in mainland China. Therefore, CGDPA product can be used as the observed data for the baseline period of this study. There are 15 rainfall stations in our study area, as shown in Figure 1.

3.2 NEX - GDDP CMIP5 data

This model uses the first global ultra-high resolution statistical downscaling climate assessment NEX-GDDP dataset released by NASA in June 2015. The dataset includes daily maximum and minimum temperature

and precipitation data for two typical concentration paths (RCP4.5 and RCP8.5). Its spatial resolution is 0.25°× 0.25°(Thrasher and Maurer, 2012). Compared with the original CMIP5 GCMs, NEX-GDDP vastly improves the spatial resolution of GCM data, improves the estimation of the average and extreme values of past historical periods, and the predictive ability, especially for areas with complex local terrain, hence, greatly improving the data availability.

10 CMIP5 models were selected with high resolution and wide representation, and the daily precipitation and temperature data under a multi-model set by equal weight average for two scenarios were obtained. The original spatial resolution of the 10 models and the information of research institutes are listed in Table 2.

Table 2. Information on the 10 climate models used in the present analysis.

Institution	**GCM**	**Resolution(Long×Lat, Degree)**	**Country**
Centre National de Recherches Météorologiques/Centre Européen de Recherche et Formation Avancée en Calcul Scientifique (CNRM–CERFACS)	CNRM-CM5	1.40°×1.40°	French
Atmosphere and Ocean Research Institute (The University of Tokyo), National Institute for Environmental Studies, and Japan Agency for Marine-Earth Science and Technology (MIROC)	MIROC5	1.40°×1.40°	Japan
National Science Foundation, Department of Energy, National Center for Atmospheric Research	CESM-BGC	0.94°×1.25°	USA
Commonwealth Scientific and Industrial Research Organization (CSIRO) and Bureau of Meteorology (BOM), Australia	ACCESS 1.0	1.25°×1.875°	Australia
National Center For Atmospheric Research（NCAR）	CCSM4	0.94°×1.25°	USA
Commonwealth Scientific and Industrial Research Organisation in collaboration with the Queensland Climate Change Centre of Excellence(CSIRO-QCCCE), Australia	CSIRO-Mk 3.6.0	1.875° × 1.875°	Australia
Institute for Numerical Mathematics(LNM), Russia	INM-CM4	2.0°×1.5°	Russia
Institute Pierre-Simon Laplace(IPSL), France	IPSL-CM5A-MR	1.2676°×3.75°	France
Max Planck Institute for Meteorology(MPI-M), Germany	MPI-ESM-MR	1.875° × 1.875°	Germany
Meteorological Research Institute (MRI), Japan	MRI-CGCM3	1.125° × 1.125°	Japan

4 RESULTS AND ANALYSIS

4.1 Spatial variation characteristics of future extreme precipitation events

Table 3 shows the MK trends of the extreme precipitation indicators in the study area every 10 years from 2020 to 2099 on the basin scale. Figure 3 shows the spatial distribution of the trend of extreme precipitation indicators in the Ya-lung River Basin for two scenarios (compared with the CMIP5 baseline period 1961-1990).

Table 3. Trend and significance of future extreme precipitation index in the Ya-lung River Basin.

	PRCPTOT (mm/10a)	SDII (mm/(day·10a))	R1mm (day/10a)	RX5day (mm/10a)	R10mm (day/10a)	CDD (day/10a)	R95p (mm/10a)
RCP4.5	2.39*	1.67*	0.70*	2.26*	0.47*	-0.42*	0.003*
RCP8.5	4.02*	3.38*	-0.61*	4.95*	0.67*	-0.36*	0.02*

Note: The value represents slope, where the * indicates that the significance level α =0.05 is passed.

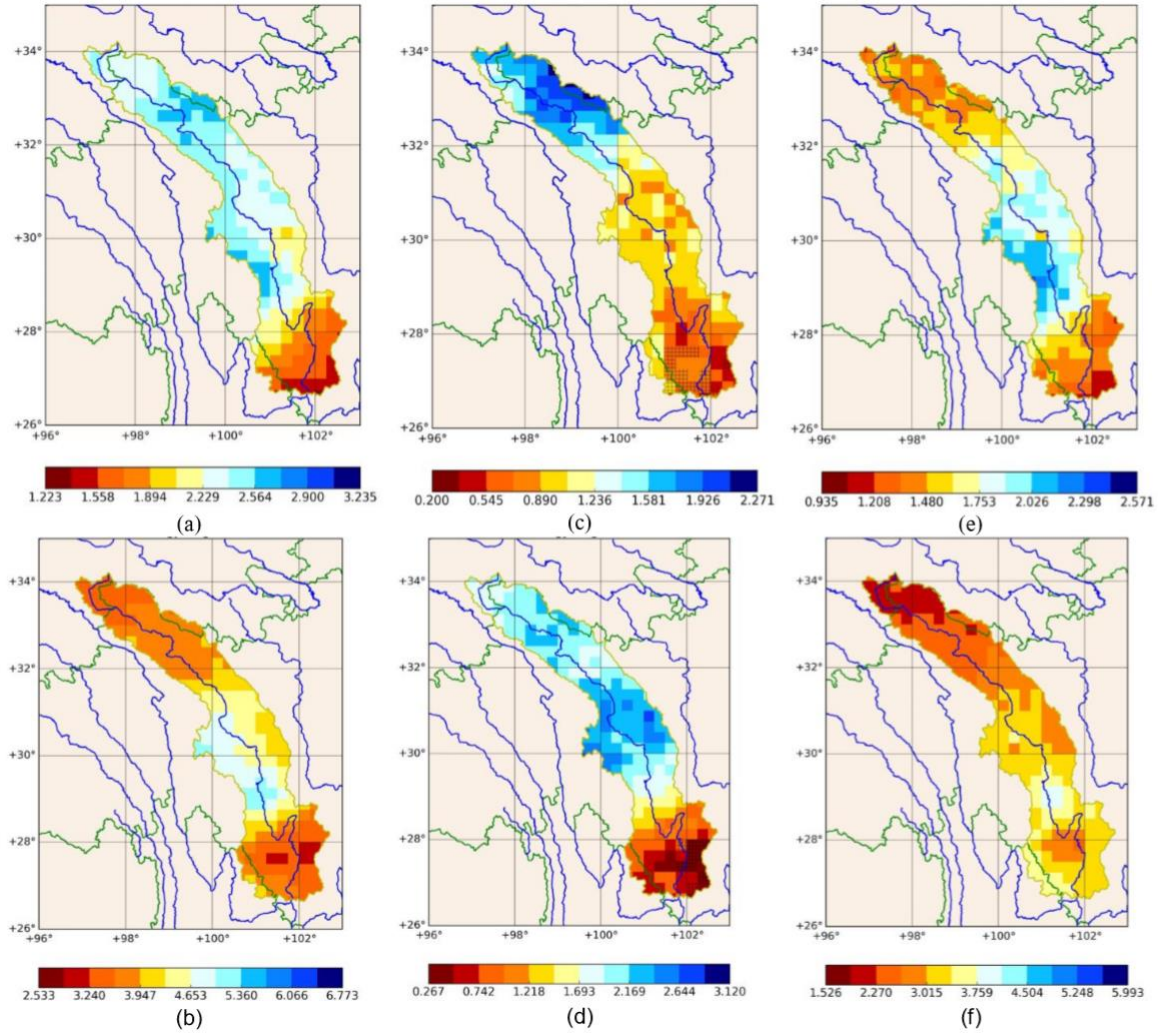

Figure 3. Spatial variation trends of annual total wet-day precipitation (RCPTOT) (a, b), number of precipitation days (R1mm) (c, d) and simple daily intensity index (SDII) (e, f) on interdecadal scales in extreme precipitation indices from 2020 to 2099. (The pictures of a, c, and e are for the RCP4.5; b, d, and f are for the RCP8.5). A positive value represents an increase in trend, a negative value represents a decrease in trend, and a black grid mark represents a trend test where the cell does not pass the MK significance level α = 0.05.

In both climate change scenarios, the PRCTOT on the basin scale shows a significant increase trend, which is 2.39 mm/10a and 4.02 mm/10a in RCP4.5 and RCP8.5 respectively. In the spatial distribution, the distribution of PRCTOT under RCP4.5 is centered on the southeastern regions and gradually increases to the northwestern regions. The maximum increase reaches 3.23 mm/10a. The lowest increase point was in the southeast corner, with a value of 1.23 mm/10a. While the change pattern of PRCTOT under RCP 8.5 is different from that of RCP 4.5. The most obvious increase is in the central of the basin, and the increase range of PRCTOT in other areas is lower than that in the center. In RCP 8.5, the increase range of PRCTOT is higher than that of RCP 4.5, ranging from 2.53 mm/10a to 6.77 mm/10a.

For R1mm, it shows an overall significant increase in the number of precipitation days in the basin scale under RCP4.5. In the basin scale under RCP8.5, the number of precipitation days shows a significant decrease. On the 0.25° pixel scale, the northwestern part of Ya-lung River Basin has the highest increase under RCP4.5, with the highest value being 2.271 d/10a. In the southeastern part, the increase is slightly lower and the trend of increase is insignificant especially near the watershed outlet. The minimum value is 0.2 d/10a. The change in the grid scale under the RCP8.5 scenario is more consistent with the RCP4.5 scenario, with the most significant increase in the upstream of the basin and the highest value being 3.12 d/10a. R1mm in the northwest outlet of the basin increases the least, at 0.27 d/10a.

In theory, SDII is jointly determined by PRCTOT and R1mm. In both scenarios, SDII shows a significant increase trend on the basin scale. In RCP8.5, on the spatial scale, the changing trend of SDII is consistent with that of PRCTOT. The maximum value is located in the middle of the basin, which is 5.99 mm/(day·10a); and the minimum value is located in the northwest region, which is 1.53 mm/(day·10a). However, in RCP4.5, the spatial

distribution of SDII and PRCTOT is inconsistent, and SDII increases more in the central region, with a maximum of 2.57 mm/(day·10a); and the minimum value is located in the basin outlet, which is 1.53 mm/(day·10a).

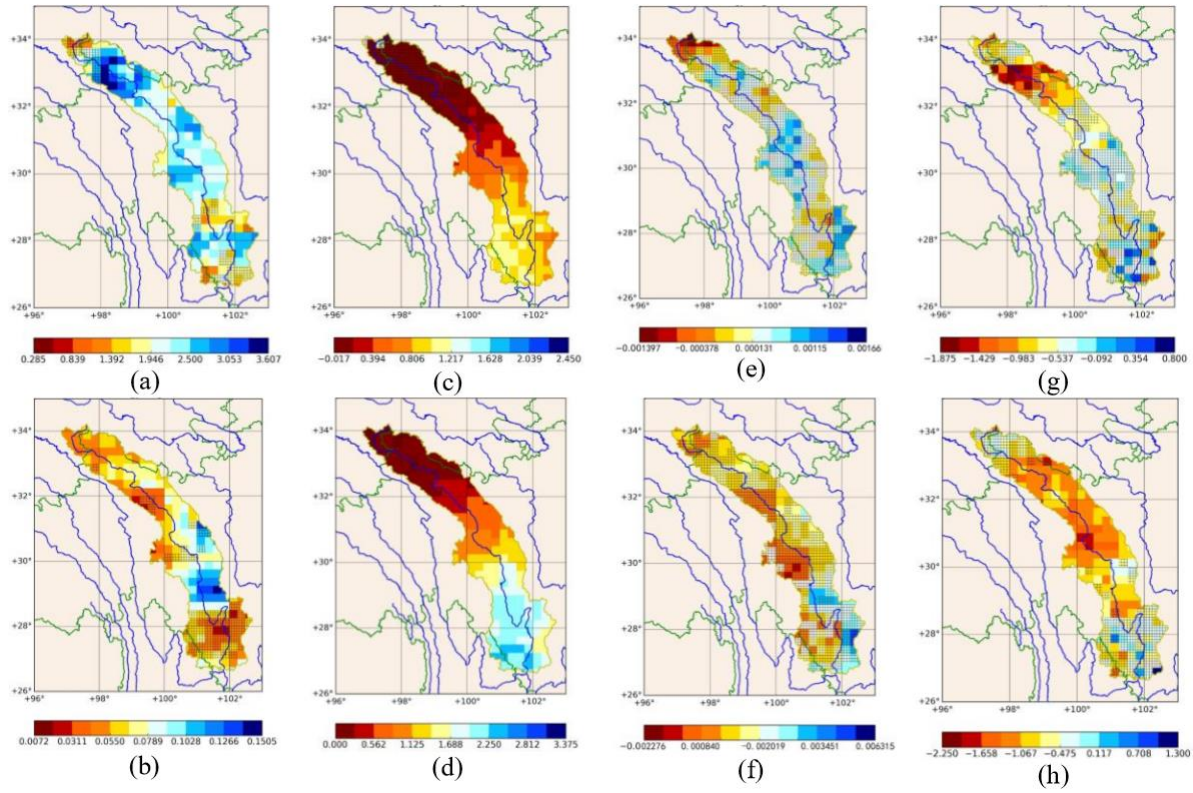

Figure 3. Spatial variation trends of maximum 5-day precipitation amount (RX5day) (a, b), number of heavy precipitation days (R10mm) (c, d), strong precipitation events (R95p) (e, f), and consecutive dry days CDD (g, h) on interdecadal scales in extreme precipitation indices from 2020 to 2099. (The pictures of a, c, e, and g are for RCP4.5; b, d, f, and h are for RCP8.5). A positive value represents an increase in trend, a negative value represents a decrease in trend, and a black grid mark represents a trend test in which the cell does not pass the MK significance level α = 0.05.

In both RCP4.5 and RCP8.5, RX5day shows a significant increase trend in the watershed, which is 2.26 mm/10a and 4.95 mm/10a respectively. In RCP4.5, RX5day increases to 2.0 mm/10a or more in most part of the basin. The linear increase at the top of the northwestern part is 3.607 mm/10a. RX5day increases less in the southeast and does not pass the significance test, with a minimum value of 0.285 mm/10a. In RCP8.5, except the southeast, central and a few grids scattered in the north, all other regions pass the significance test on spatial scale. There is a large increase trend in the southeastern part of the central region, the maximum being 0.1505 mm/10a; and there is a small increase in the northwest region, the minimum being 0.0072 mm/10a.

On the basin scale, R10mm shows a significant increase trend in both RCP4.5 and RCP8.5, which are 0.47 d/10a and 0.67 d/10a respectively. In space, the R10mm under RCP4.5 has the most obvious increase in the southeastern parts and pass the significance test, up to 2.45 d/10a. In RCP8.5, the trend in almost all grids increase significantly, and the increase trend is higher than that in RCP4.5, with the southeastern region being the most significant region with a maximum increase of 3.375 d/10a.

R95P displays obvious growths in both scenarios on the basin scale. In RCP4.5, R95P did not pass the significance test on all grids, and there was a large growth trend at the exit of the central and river basins, with a maximum of -0.00166mm/10a. At the top of the northwest, there is a decreasing trend with a maximum range of -0.001397/10a. In RCP8.5, R95P did not pass the significance test in few areas, and decreased in the central grid of the basin with the minimum value of -0.002276 /10a. The maximum increase appeared at the outlet of the basin with the maximum value of 0.006315 /10a.

The essence of R5D, R10 and R95p is to describe the extreme precipitation, while CDD indicates the maximum number of consecutive days without precipitation within the year. Therefore, unlike the above three extreme indicators, CDD is a time indicator of drought and the future changes of CDD are complex. At the basin scale, CDD shows a decreasing trend in both RCP4.5 and RCP8.5. However, for the spatial scale, the distribution of CDD in the Ya-lung River Basin is highly spatially heterogeneous, but show an increasing trend in the southeastern area. The maximum increase is 0.8 d/10a and 1.3d/10a in RCP 4.5 and 8.5, respectively. Most of the grids did not pass the significance test in RCP4.5.

Based on the above analysis, it can be concluded that on the basin scale, all extreme precipitation indicators show significant trends, with CDD and R1mm in RCP8.5 scenarios decreasing, and all the other indicators increasing. On the spatial scale, all indicators are distributed differently in different scenarios and there is no obvious regularity, indicating that the sensitivity of Ya-lung River Basin to climate change shows obvious spatial heterogeneity.

However, the above extreme precipitation indices can only represent the changing trend of specific hydrological variables, and does not represent the change of the overall precipitation in the Ya-lung River Basin. Therefore, univariate and multivariate trend analysis is required for specific hydrological variables.

4.2 Estimation of future precipitation and runoff changes

After verifying the applicability of CREST model in the Ya-lung River Basin, the model is run to simulate the changing process of runoff in the two scenarios. To obtain the changes of precipitation and runoff in each interdecadal period relative to the baseline period (2005–2014), the future research period 2020–2099 is divided into three sub-periods: short-term, medium-term, and long-term. The short-term is 2020–2029 and 2030–2039, the medium term is 2040–2049, 2050–2059, and 2060–2069, and the long-term is 2070–2079, 2080–2089, and 2090–2099. Then, the monthly and seasonal analysis is carried out to compare with the baseline period. Finally, univariate and multivariate trend analysis of precipitation and runoff is used to analyze the changing characteristics of runoff in the Ya-lung River Basin under future RCP4.5 and 8.5 climate changing scenarios.

4.2.1 Verification of CREST model

Daily runoff simulation of Ertan Hydrological Station is conducted for the calibration period from 1996 to 2004 and the validation period from 2006 to 2014. The results are shown in Fig. 4. According to the daily runoff simulation results, CREST model can accurately simulate the flood peak and the time when the peak appears during the calibration period. Due to the warm-up period for the model is set at 1996, which leads to an obvious underestimation of runoff at the beginning period of 1996. However, during the verification period, CGDPA has a significant underestimation in 2014. Combined with the example of model parameter fitting (Zhong Z et al.), the reason is that the parameters appear to be over-fitting, resulting in the simulation of the validation period is inferior compared to the calibration period. According to Table 4, Nash coefficient is 0.82 and 0.60, R2 is 0.84 and 0.85, bias is -2.05% and 3.01% respectively in the calibration and validation periods. In summary, CREST can better simulate the daily runoff of the Ya-lung River Basin during the calibration and validation periods. It is feasible to apply this model for climate change impact simulation and assessment.

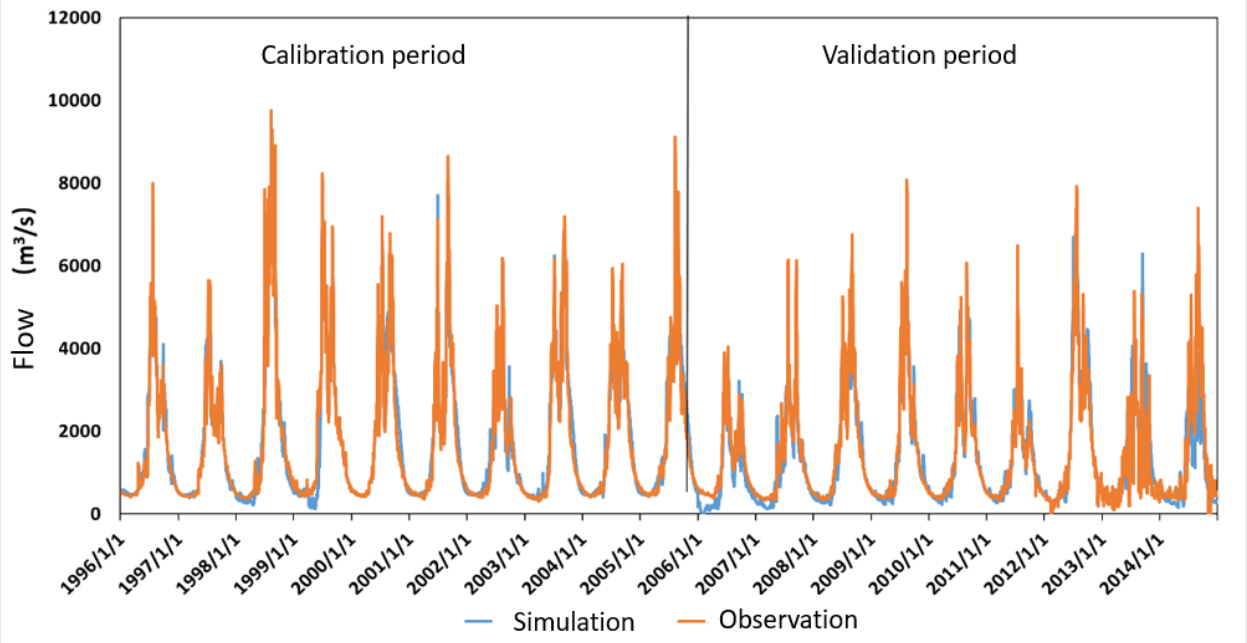

Figure 4. Calibration and verification of runoff in the Ya-lung River Basin.

Table 4. Calibration and verification results of daily runoff at the Ertan Hydrological Station in the Ya-lung River Basin.

	Nash	R^2	Bias(%)
Calibration period	0.83	0.84	-2.05

Validation period	0.84	0.85	3.01

4.2.2 Interdecadal variations of future precipitation and runoff

The daily precipitation and runoff of eight interdecadal periods are accumulated to get their respective total amount, and then the multi-year average value of each interdecadal period is calculated and compared with that of the baseline period. As shown in Fig. 5, in RCP4.5, the precipitation in 2020–2099 shows a slow increase on the interdecadal scale. The percentage change of precipitation in different interdecadal periods relative to the baseline period is shown in Fig. 6. Precipitation is gradually rising, but by the end of the 2090s it is still below the precipitation of the baseline period. In RCP 4.5, the runoff change shows a jagged upward trend, and the percentage change with the baseline period reaches the maximum of 32.44% in the 2080s (Fig. 6). In summary, under RCP4.5, precipitation has a large variation in the short term, while the runoff varies significantly in the long term.

In RCP8.5, the multi-year average precipitation and runoff in the eight interdecadal periods show increasing trends, and the changing range is larger than that under RCP4.5 (Fig. 5). In Fig. 6, precipitation and runoff increase continuously under RCP8.5, and the range of change relative to the baseline period also gradually increases. In the short term, the average increase of precipitation is 7.07%, and the average increase of runoff is 31.03%. In the medium term, the average increase in precipitation and runoff reaches 2.30% and 43.44%, respectively. At the end of the 21st century, the average increase in precipitation and runoff reaches the highest, at 10.98% and 56.27% respectively.

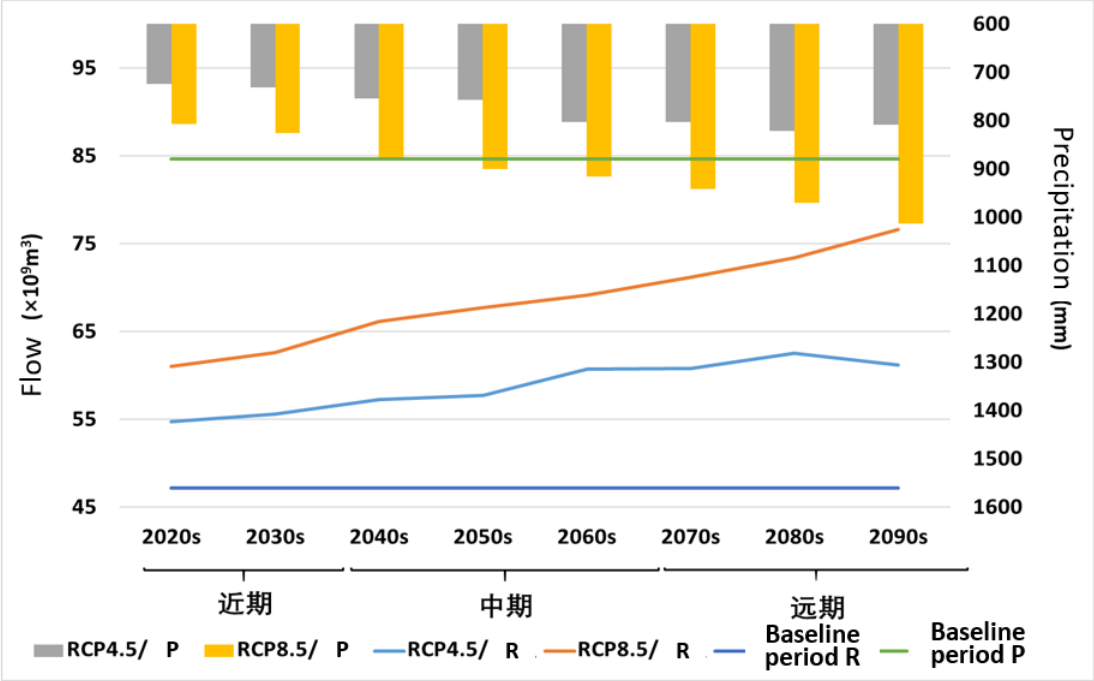

Figure 5. Precipitation/runoff change (The yellow/grey bars represent the multi-year average precipitation under RCP8.5/RCP4.5 over different interdecadal periods respectively. The orange/blue fold line represent the multi-year average runoff under RCP8.5/RCP4.5 over different interdecadal periods respectively. The multi-year average precipitation in the baseline period is 879.10 mm and the multi-year average runoff in the baseline period is 47.16×10^9 m^3).

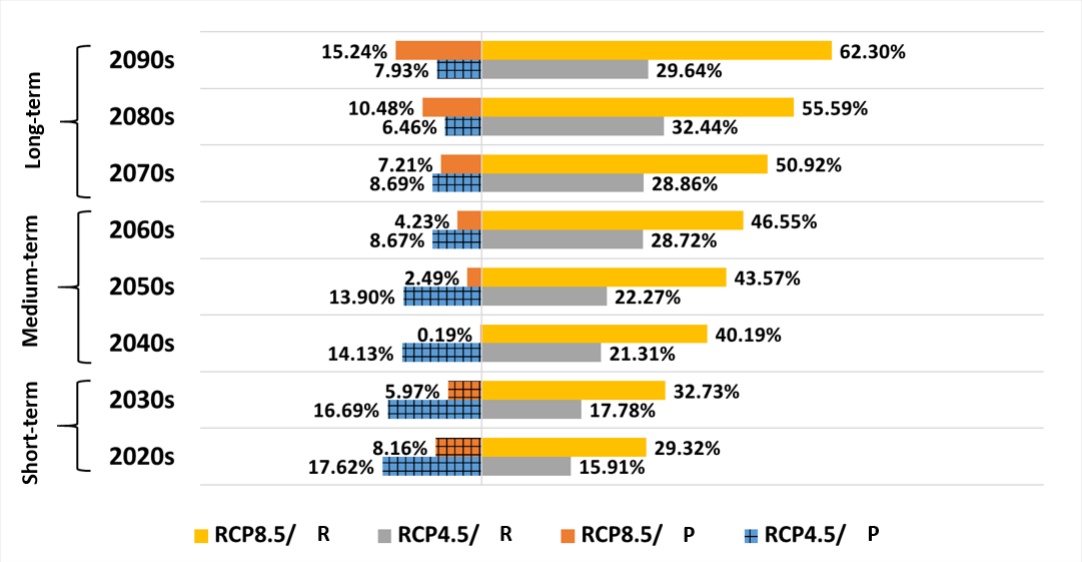

Figure 6. Percentage change of precipitation/runoff in each interdecadal period relative to the baseline period (The yellow/grey bars represent the percentage change of runoff in each interdecadal period relative to the baseline period (2005–2014) under RCP8.5/RCP4.5. The orange/blue bars represent the percentage change of precipitation in each interdecadal period relative to the baseline period (2005–2014) under RCP8.5/RCP4.5.The bar with black crosses means decrease relative to the base period (2005-2014)).

4.2.3 Seasonal variations of future precipitation and runoff

It can be seen from Table 5 that the precipitation in the RCP4.5 scenario shows a decrease compared to the baseline period, with the largest variation in winter, the second large variation in spring, and the smallest increase in summer. In RCP4.5, except for the decrease runoff in winter, runoff in other seasons all increase compared to the baseline period, but the increase in spring is only 0.73%. In the RCP8.5 scenario, precipitation grows to 11.22% in the summer compared to the baseline period, while declines in the other three seasons, with the largest decrease in winter, which is 93.79%. Except for the winter, the runoff in RCP8.5 shows a rising trend compared to the baseline period and reaches the maximum in summer, at 71.02%. It can be concluded that precipitation and runoff are abundant in RCP8.5 than in the RCP4.5 scenario, but both of them have rare rains in winter, and thus runoff is reduced. Therefore, the relevant departments should store water in advance in the future.

Table 5. Simulation results of precipitation and runoff in different seasons under different climate scenarios in the future.

RCPs	Precipitation（%）				Runoff（%）			
	Spring	Summer	Autumn	Winter	Spring	Summer	Autumn	Winter
4.5	-12.24	-9.96	-10.15	-94.20	0.73	40.74	36.93	-80.57
8.5	-4.86	11.22	-3.48	-93.79	7.06	71.02	53.29	-80.26

4.3 Multivariate trend analysis of future precipitation and runoff

Hydrological processes contain multiple elements. If only one variable is considered when analyzing a hydrological process, it will likely yield the wrong trend analysis results (Chebana et al., 2013). The results of univariate and multivariate trend analysis can be comprehensively applied to obtain the most complete and accurate conclusion of the overall trend of hydrological process (Chebana et al., 2011). According to the indicators selected by Ye et al. (2014) and Wang et al. (2015), the total annual rainfall (P), the annual maximum daily rainfall (Pmax), annual maximum peak flow (Max), and the annual maximum 7-day flood (Max7d) of Ertan Hydrological Station in the next 80 years are estimated. To ensure the continuity and independence of data in Mann-Kendall test, a data pre-whitening program is implemented to eliminate sequence correlation before applying the Mann-Kendall test, and then the univariate and multivariate trends are analyzed. The results are shown in Tables 6 and 7.

Table 6. Univariate trend analysis.

RCP	Univariate	Z Value	Trend
RCP4.5	Total annual rainfall (P)	-2.56 *	-
	Annual maximum daily rainfall (Pmax)	-2.19*	-
	Annual maximum peak flow (Max)	-2.68*	-
	Annual maximum 7-day flood (Max7d)	-2.66*	-

RCP8.5	Total annual rainfall (P)	-2.38*	-
	Annual maximum daily rainfall (Pmax)	-2.03*	-
	Annual maximum peak flow (Max)	-2.29*	-
	Annual maximum 7-day flood (Max7d)	-2.28*	-

Note: The significance level α is 0.05, the threshold is 1.96, + represents the increasing trend, - represents the decreasing trend, * denotes the trend is significant, and without* denotes the trend is insignificant.

Table 7. Multivariate trend analysis.

RCP	Multivariate	CIT	CST
RCP4.5	Total annual rainfall (P), Annual maximum daily rainfall (Pmax)	23.23*	4.80*
	Annual maximum peak flow (Max), Annual maximum 7-day flood (Max7d)	20.53*	4.53*
RCP8.5	Total annual rainfall (P), Annual maximum daily rainfall (Pmax)	14.46*	3.69*
	Annual maximum peak flow (Max), Annual maximum 7-day flood (Max7d)	23.39*	4.84*

Note: The significance level α is 0.05, the CIT threshold is 5.99, and the CST threshold is 1.96. * denotes a significant trend, without* denotes the trend is insignificant.

Table 6 shows that under RCP4.5, the trend of total annual rainfall (P) and annual maximum daily rainfall (Pmax) will decrease and pass the significant test, which means the annual precipitation and extreme precipitation events in the Ya-lung River Basin will be significantly reduced in the next 80 years. In the multivariate trend analysis of Table 7, the CIT and CST results of P and Pmax all shows significant changes, indicating that the overall precipitation in the Ya-lung River Basin has a significant decreasing trend in RCP4.5. Compared with the univariate trend analysis, it can be considered that in the future scenario, the precipitation in the Ya-lung River basin will decrease overall during the year, and the extreme value of extreme precipitation events will decline with the precipitation.

Similarly, in the unvariate trend analysis under RCP4.5, annual maximum peak flow (Max) and annual maximum 7-day flood (Max7d) both display significant decreasing trends in the next 80 years. Meanwhile, in the multivariate trend analysis, Max and Max7d also pass the CIT and CST test, indicating that there is a significant decreasing trend of multivariable. Therefore, it shows that the runoff in the Ya-lung River Basin has a significant reduction trend in RCP4.5 scenario. Under the situation that the precipitation is seriously less and the rivers are seriously dry, it is necessary to pay more attention to strengthen water conservancy construction and comprehensively improve the capacity of drought disaster prevention.

The results in RCP8.5 is similar to that in RCP4.5. Referring to the results of the univariate trend analysis, it shows that the future runoff of the Ya-lung River Basin shows a significant decrease trend both in the whole and in the local period.

5 CONCLUSION

In this study, a one-way connection system between climate and CREST hydrological model was established in the Ya-lung River Basin. After verifying the applicability of the model, the trend and significance of extreme precipitation indicators in the study area on the basin and grid scales were analyzed. Finally, the changes in precipitation and runoff in the Ya-lung River basin under different climate change scenarios were predicted. The main conclusions are as follows:

(1) According to the trend and significance analysis of extreme precipitation indices in the Ya-lung River Basin on the basin and grid scales between 2020 and 2090, it can be seen that the total annual precipitation (PRCPTOT), days of heavy precipitation (R10mm), intensity of precipitation (SDII), and maximum continuous 5-day precipitation (RX5day) on the basin scale show a significant increase trend in both scenarios. Spatially, the consecutive dry days (CDD) in the two scenarios show insignificant decreasing trend, indicating that the drought situation in the Ya-lung River Basin will be alleviated in the future. According to R95P, there will be no significant change in the future extreme precipitation in the two scenarios, but there will be different degrees of increase or decrease in some areas.

(2) CREST model was used to simulate the daily runoff of the Ertan hydrological station in the Ya-lung River Basin. The results show that the Nash efficiency coefficient (0.83, 0.84), the deterministic coefficient (0.84, 0.88), and the relative error (-2.05%, 3.01%) of CREST model in the calibration and verification periods all meet the accuracy requirements, which proves that CREST can accurately simulate the runoff process in the study area and has good applicability in the Ya-lung River Basin.

(3) Based on the climate prediction data of NASA-GDDP CMIP5 and Hargreaves-Samani (HS) method, the daily runoff in 2020–2099 is obtained by running CREST. The prediction results show that precipitation and runoff will increase in different degrees in both scenarios, and RCP8.5 scenario has more precipitation and runoff than RCP4.5 for the same period. In both scenarios, the increase in precipitation is mainly concentrated in winter, while the growth of runoff is mainly concentrated in summer and autumn.

(4) Through the univariate and multivariate MK trend analysis, the results show that there will be a significant decrease trend for future precipitation and runoff in the Ya-lung River Basin between 2020 and 2099. The multivariable of annual maximum peak flow (Max) and annual maximum 7-day flood (Max7d) also show a significant decrease trend

Due to the certain uncertainties in global climate model and CREST (Teng et al. (2012)). Therefore, in future research, multiple models and emission scenarios can be selected and the impact of human activities can be considered to better understand the response of climate to changes in hydrology and water resources. Although a panoramic analysis of the 21st century was carried out, the IPCC has recently issued the latest special report on a 1.5℃ global temperature rise. The next step research should be concentrated on the water resources situation of the Ya-lung River Basin under a global target of 1.5℃ and 2.0℃ temperature rise.

ACKNOWLEDGEMENTS
This work is funded by National Key R&D Program of China (Grant No. 2018YFC0407701).

REFERENCES

IPCC. Climate Change 2007: The Physical Science Basis, Contribution of Working Group Ⅰ to the Fourth Assessment Report of the Intergovemmental Panel on Climate Change [R] .Cambridge University Press,2007.

IPCC. Climate Change 2013 :The Physical Science Basis, Contribution of Working Group 1 to the Fifth Assessment Report of the lntergovernmental Panel on Climate Change [R].Cambridge University Press, 2013.

Chen J, Gao C, Zeng X, et al. Assessing changes of river discharge under global warming of 1. 50C and 20C in the upper reaches of the Yangtze River Basin: Approach by using multiple 一 GCMs and hydrological models[J].Quaternary lnternationa1,2017 (453) :63-73.

Jiang T, Chen Y Q, Xu C Y, et al. Comparison of hydrological impacts of climate change simulated by six hydrological models in the Dongjiang Basin, South China [J]. Journal of Hydrology, 2007, 336(3/4): 316-333.

Xu Z X, Zhao F F, Li J Y. Response of streamflow to climate change in the headwater catchment of the Yellow River Basin [J]. Quaternary International, 2009, 208 (1/2): 62-75.

Vaze, J. , Teng J. . Future climate and runoff projections across New South Wales, Australia: results and practical applications[J]. HYDROLOGICAL PROCESSES, 2011,25(1): 18-35.

Yu P S, Yang T C, Wu C K. Impact of climate change on water resources in southern Taiwan [J]. Journal of Hydrology,2002,260(1/4): 161-175.

Franczyk J ,Chang H . The effects of climate change and urbanization on the runoff of the Rock Creek basin in the Portland metropolitan area, Oregon, USA[J]. HYDROLOGICAL PROCESSES,2009,23(6): 805-815.

Silberstein RP, Aryal SK, Durrant, J ,et al. Climate change and runoff in south-western Australia[J]. JOURNAL OF HYDROLOGY, 2012,475: 441-455.

Wang G Q, Zhang J Y, Liu J F, et al. The sensitivity of runoff to climate change in different climatic regions in China[J]. ADVANCES IN WATER SCIENCE, 2011,22(3): 307-314.

Chen J X, Xia J , Zhao C S, et al. The mechanism and scenarios of how mean annual runoff varies with climate change in Asian monsoon areas[J]. JOURNAL OF HYDROLOGY, 2014, 517: 595-606.

Liu S Y, Zhang Y, Zhang Y S, et al. Estimation of glacier runoff and future trends in the Yangtze River source region, China[J].2009,55(109): 353-362.

Li L, Shen H Y, Dai S, et al. Response of runoff to climate change and its future tendency in the source region of Yellow River[J]. JOURNAL OF GEOGRAPHICAL SCIENCES, 2012,22(3): 431-440.

Yuan Z, Yan D H, Yang Z Y, et al. Attribution assessment and projection of natural runoff change in the Yellow River Basin of China[J]. MITIGATION AND ADAPTATION STRATEGIES FOR GLOBAL CHANGE, 2018,23(1): 27-49.

Yuan Z, Xu J J, Wang Y Q. Projection of Future Extreme Precipitation and Flood Changes of the Jinsha River Basin in China Based on CMIP5 Climate Models[J]. INTERNATIONAL JOURNAL OF ENVIRONMENTAL RESEARCH AND PUBLIC HEALTH,2018,15(11).

Supari; Tangang F, Fredolin L,et al. Observed changes in extreme temperature and precipitation over Indonesia[J]. INTERNATIONAL JOURNAL OF CLIMATOLOGY, 2017,37(4): 1979-1997.

Mingxiang Y, Hao W, Yunzhong J, Xiaohui L, Jiaojian S. Preliminary evaluation of wind energy resources in the Yalong River Basin based on numerical simulation[J]. Journal of Tsinghua University(Science and Technology), 2018, 58(01): 101-107.

Tang G Q, Zeng Z Y, Long D, et al. Statistical and Hydrological Comparisons between TRMM and GPM Level-3 Products over a Midlatitude Basin: Is Day-1 IMERG a Good Successor for TMPA 3B42V7?[J]. JOURNAL OF HYDROMETEOROLOGY, 2016,17(1):121-137.

KHAN S I, ADHIKARI P, HONG Yang, et al. Hydroclimatology of Lake Victoria region using hydrologic model and satellite remote sensing data[J]. Hydrology and Earth System Sciences, 2011, 15 (1):107-17.

KHAN S I, HONG Yang, WANG Jiahu, et al. Satellite remote sensing and hydrologic modeling for flood inundation mapping in Lake Victoria basin: Implications for hydrologic prediction in ungauged basins [J]. Geoscience and Remote Sensing, IEEE Transactions on, 2011，49 (1):85 -95.

WU Huan, ADLER R F, HONG Yang, et al. Evaluation of global flood detection using satellite-based rainfall and a hydrologic model[J]. Journal of Hydrometeorology, 2012, 13 (4):1268-1284.

Nilawar AP, Waikar ML. Use of SWAT to determine the effects of climate and land use changes on streamflow and sediment concentration in the Purna River basin, India[J]. ENVIRONMENTAL EARTH SCIENCES, 2018,77(23).

Huaijun W, Yinping Pm Zhongshen C. Temporal and Spatial Variation Characteristics of Extreme Temperature and Precipitation in the Huaihe River Basin from 1960 to 2014 [J]. GEOSCIENCE, 2017, 37(12): 1900-1908.

Changchun C, Yuqing Z, Lachun W, Tiezhu Y, Jie S. Temporal and Spatial Variations of Extreme Precipitation in Jiangxi Province Based on RClimDex Model[J]. China Rural Water and Hydropower, 2013(11): 41-45.

Filahi S; Tanarhte M ; Mouhir L,et al. Trends in indices of daily temperature and precipitations extremes in Morocco[J]. THEORETICAL AND APPLIED CLIMATOLOGY, 2016, 124(3-4): 959-972.

Shen Y, Zhao P, Pan Y, et al. A high spatiotemporal gauge-satellite merged precipitation analysis over China[J]. Journal of Geophysical Research Atmospheres, 2014, 119(6):3063-3075.

Shen Y, Xiong A Y. Validation and comparison of a new gauge-based precipitation analysis over mainland China[J]. INTERNATIONAL JOURNAL OF CLIMATOLOGY,2016,36:252-265.

Thrasher, B., E. P. Maurer, C. Mckellar, and P. B. Duffy (2012), Technical Note: Bias correcting climate model simulated daily temperature extremes with quantile mapping, Hydrology & Earth System Sciences, 16(9), 3309-3314.

Zhong Z, Zheng L, Zheng Z, et al. CamStyle: A Novel Data Augmentation Method for Person Re-Identification[J]. IEEE TRANSACTIONS ON IMAGE PROCESSING, 2019,28(3): 1176-1190.

Chebana F., Ouarda T.B.M.J., Duong T.C. Testing for multivariate trends in hydrologic frequency analysis [J]. Journal of Hydrology, 2013,486:519-530.

Lei Y, Jianzhong Z, Xiaofan Z, Lu C, Jun G, Hairong Z. Applied Research on Hydrological Multivariate Trend Analysis [J]. Hydrology, 2014, 34(06):33-39.

Le W, Dedi L, Tianyuan L, Jiasheng W, Liny L. Analysis of Precipitation Trend in Beijiang River Basin Based on Multivariate M-K Test [J]. Hydrology, 2015, 35(04):85-90.

Teng, J., Vaze, J., Chiew, F.H.S., Wang, B., Perraud, J., 2012. Estimating the relative uncertainties sources from GCMs and hydrological models in modeling climate change impact on runoff. J. Hydrometeor. 13, 122–139.